SUPPORTING INFORMATION

for

The global repair profile of human alkyladenine DNA glycosylase on nucleosomes reveals DNA packaging effects

Erin E. Kennedy,[a] Chuxuan Li,[b] and Sarah Delaney[a,b]*
* sarah_delaney@brown.edu

[a]Department of Molecular Biology, Cell Biology, and Biochemistry, Brown University, Providence, RI 02912, United States

[b]Department of Chemistry, Brown University, Providence, Rhode Island 02912, United States

Table of Contents

Scheme S1. Widom 601 sequences.
I and J strand designations are based on the crystal structure of Vasudevan, *et al*. for the Widom 601 NCP.[1]

I strand:

5′-ATC AGA ATC CCG GTG CCG AGG CCG CTC AAT TGG TCG TAG ACA GCT CTA GCA CCG CTT AAA CGC ACG TAC GCG CTG TCC CCC GCG TTT TAA CCG CCA AGG GGA TTA CTC CCT AGT CTC CAG GCA CGT GTC AGA TAT ATA CAT CGA T

J strand:

5′- ATC GAT GTA TAT ATC TGA CAC GTG CCT GGA GAC TAG GGA GTA ATC CCC TTG GCG GTT AAA ACG CGG GGG ACA GCG CGT ACG TGC GTT TAA GCG GTG CTA GAG CTG TCT ACG ACC AAT TGA GCG GCC TCG GCA CCG GGA TTC TGA T

Scheme S2. Ligation strategy for complementary 145 mer oligonucleotides lacking damage.

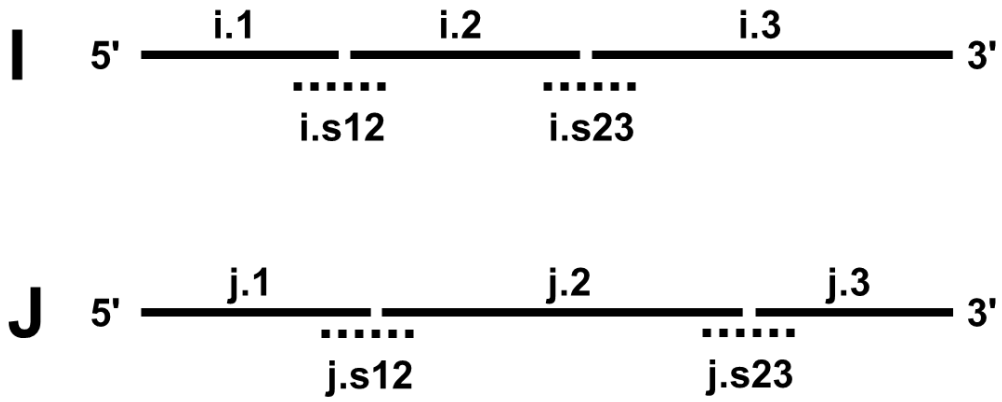

Component	Length	Sequence (5' to 3')
i.1	35mer	ATCAGAATCCCGGTGCCGAGGCCGCTCAATTGGTC
i.2	45mer	GTAGACAGCTCTAGCACCGCTTAAACGCACGTACGCGCTGTCCCC
i.3	65mer	CGCGTTTTAACCGCCAAGGGGATTACTCCCTAGTCTCCAGGCACGTGTCAGATATATACATCGAT
i.s12	32mer	GTGCTAGAGCTGTCTACGACCAATTGAGCGGC
i.s23	26mer	GGCGGTTAAAACGCGGGGGACAGCGC
j.1	45mer	ATCGATGTATATATCTGACACGTGCCTGGAGACTAGGGAGTAATC
j.2	65mer	CCCTTGGCGGTTAAAACGCGGGGGACAGCGCGTACGTGCGTTTAAGCGGTGCTAGAGCTGTCTAC
j.3	35mer	GACCAATTGAGCGGCCTCGGCACCGGGATTCTGAT
j.s12	30mer	TTTAACCGCCAAGGGGATTACTCCCTAGTC
j.s23	32mer	GCCGCTCAATTGGTCGTAGACAGCTCTAGCAC

Scheme S2. Ligation strategy for complementary 145 mer oligonucleotides lacking damage. Each 145 mer is assembled by the ligation of three component oligonucleotides. Components 2 and 3 are 5′-phosphorylated and combined with component 1 and two scaffold oligonucleotides s12 and s23 for annealing. Annealed strands are subsequently ligated to create the full-length strands. When global εA was in the I strand, it was annealed to the non-lesion-containing J strand. Similarly, when global εA was in the J strand, it was annealed to the non-lesion-containing I strand.

Scheme S3. Sequences of internal reference oligonucleotides.

23 mer:

5′-ATC AGA ATC CCG GTG CCG AGG CC

92 mer:

5′-ATC AGA ATC CCG GTG CCG AGG CCG CTC AAT TGG TCG TAG ACA GCT CTA GCA CCG CTT AAA CGC ACG TAC GCG CTG TCC CCC GCG TTT TAA CC

53 mer:

5′-ATC GAT GTA TAT ATC TGA CAC GTG CCT GGA GAC TAG GGA GTA ATC CCC TTG GC

Figure S1. Confirmation of εA substitutions for A in Widom 601 I and J strands.

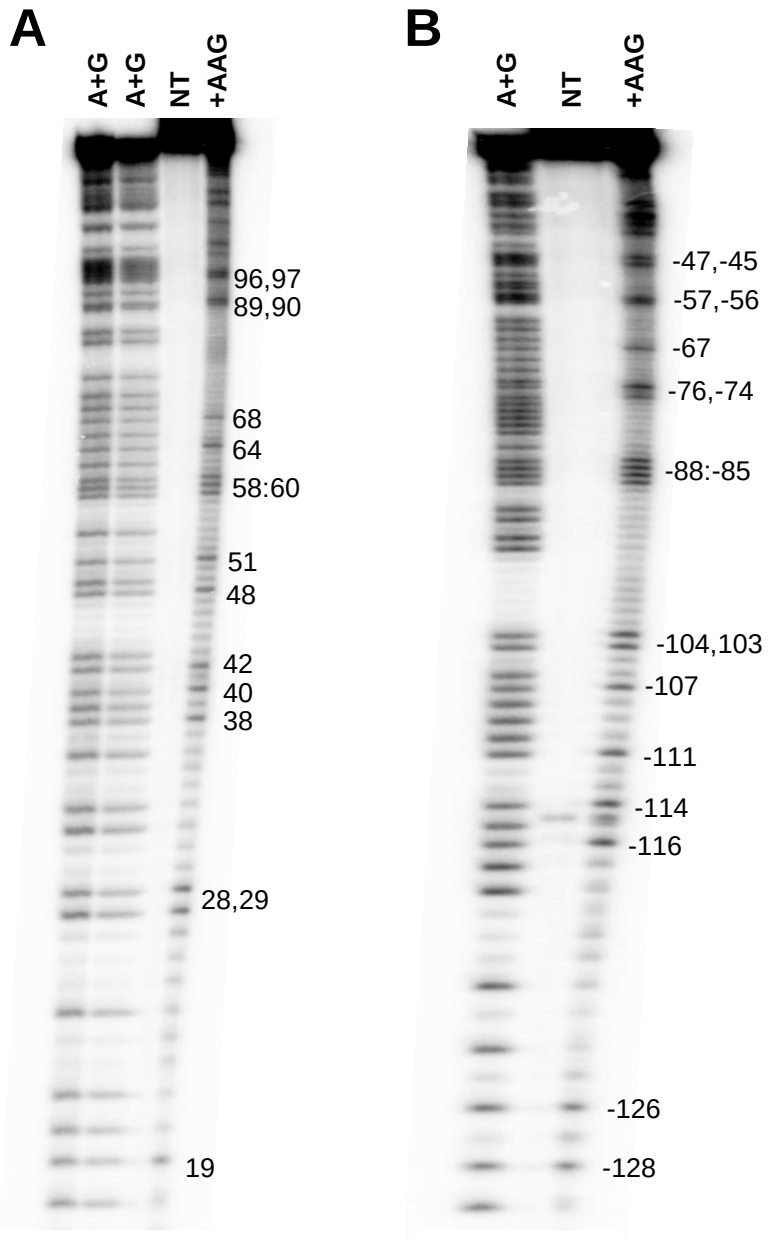

Figure S1. Confirmation of εA substitutions for A in Widom 601 I and J strands. The εA was incorporated separately in the (**A**) I and (**B**) J strands. The A+G lanes display a sequence ladder created using Maxam-Gilbert reactions using Widom 601 sequences lacking εA lesions. NT lanes show untreated I or J strand. The +AAG lanes are DNA duplexes containing εA in either the I or J strand treated with AAG for 1 h at 37 °C and quenched with the addition of NaOH to create strand breaks at AAG-generated abasic sites. In both PAGE images, the parent band was partially cropped for clarity.

Figure S2. Single-turnover time course experiments of εA excision by AAG on the I strand of DNA substrates.

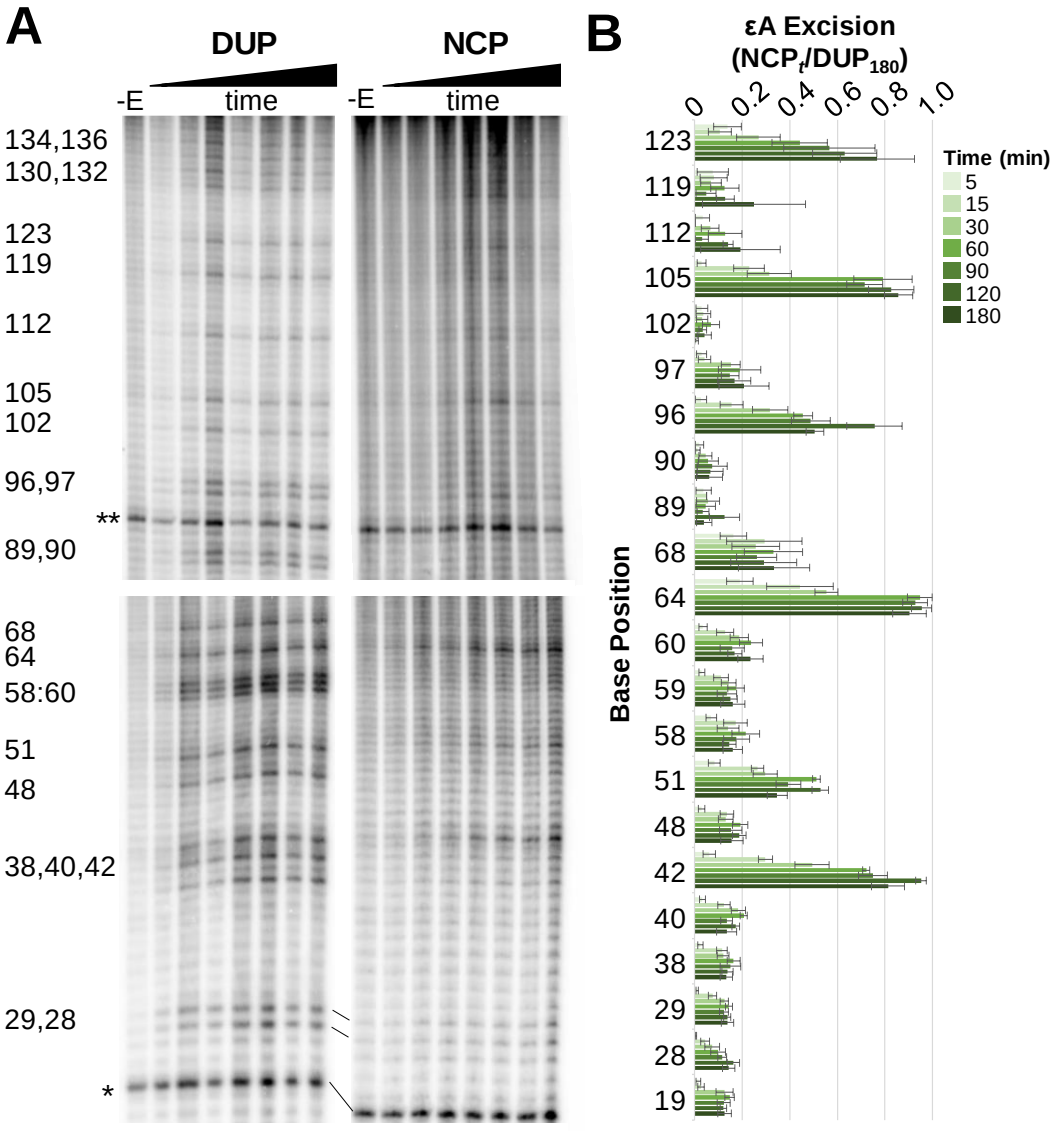

Figure S2. Single-turnover kinetic time course experiments of εA excision by AAG on the I strand of DNA substrates. (**A**) Representative PAGE gels showing εA excision from DUP (left) and NCP (right). DNA samples only treated with NaOH (-E lanes) show incidental damage from experimental conditions and sample workup. Two internal references, a 23 mer (*) and 92 mer (**), used for quantitation are indicated. Four separate gels are shown, indicated by the spaces between the images, with each gel cropped for alignment. The top two panels are aligned to show DUP and NCP data for positions 136-89. The bottom two panels are aligned to show data for positions 68-28. (**B**) Quantitation of εA excision over time on the I strand in NCPs. Error bars are calculated standard errors (n= 3-10).

Figure S3. AAG retains full activity for 180 min.

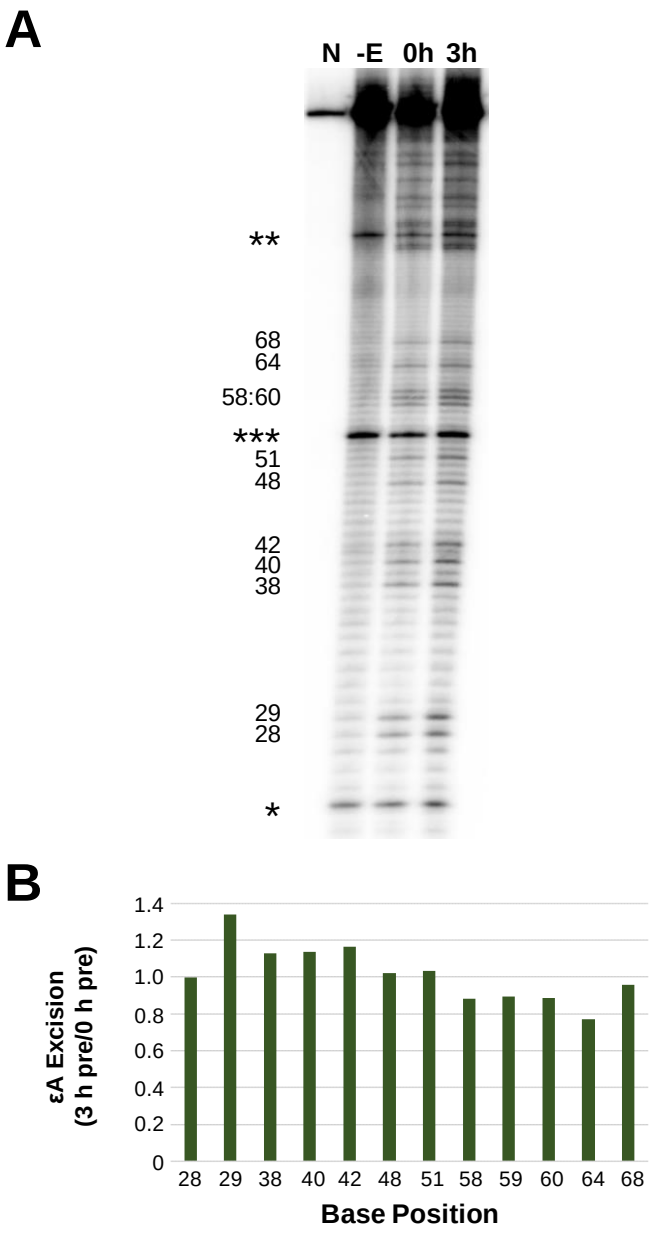

Figure S3. AAG retains full activity for 180 min. (**A**) AAG was either added directly (0 h lane) or pre-incubated at 37 °C under experimental conditions for 180 min (3 h lane) before incubation with global εAI DUP. After AAG addition, the reaction proceeded for 1 h at 37 °C before quenching with NaOH and sample workup for loading on denaturing PAGE. Three internal references, a 23 mer (*), 92 mer (**), and 53 mer (***) used for quantitation are indicated. The N lane shows the DUP sample without any treatment. The -E lane is quenched with NaOH to show any damage due to experimental conditions and workup. (**B**) Quantification of AAG activity at various positions in DUP, shown as a ratio of εA excision seen in the 3 h pre-incubation sample to the amount of εA excision seen in the 0 h sample. A ratio of 1 indicates that pre-incubation of AAG for 3 h before reaction does not influence its activity.

Figure S4. Quantitation of εA excision over time in global DUP.

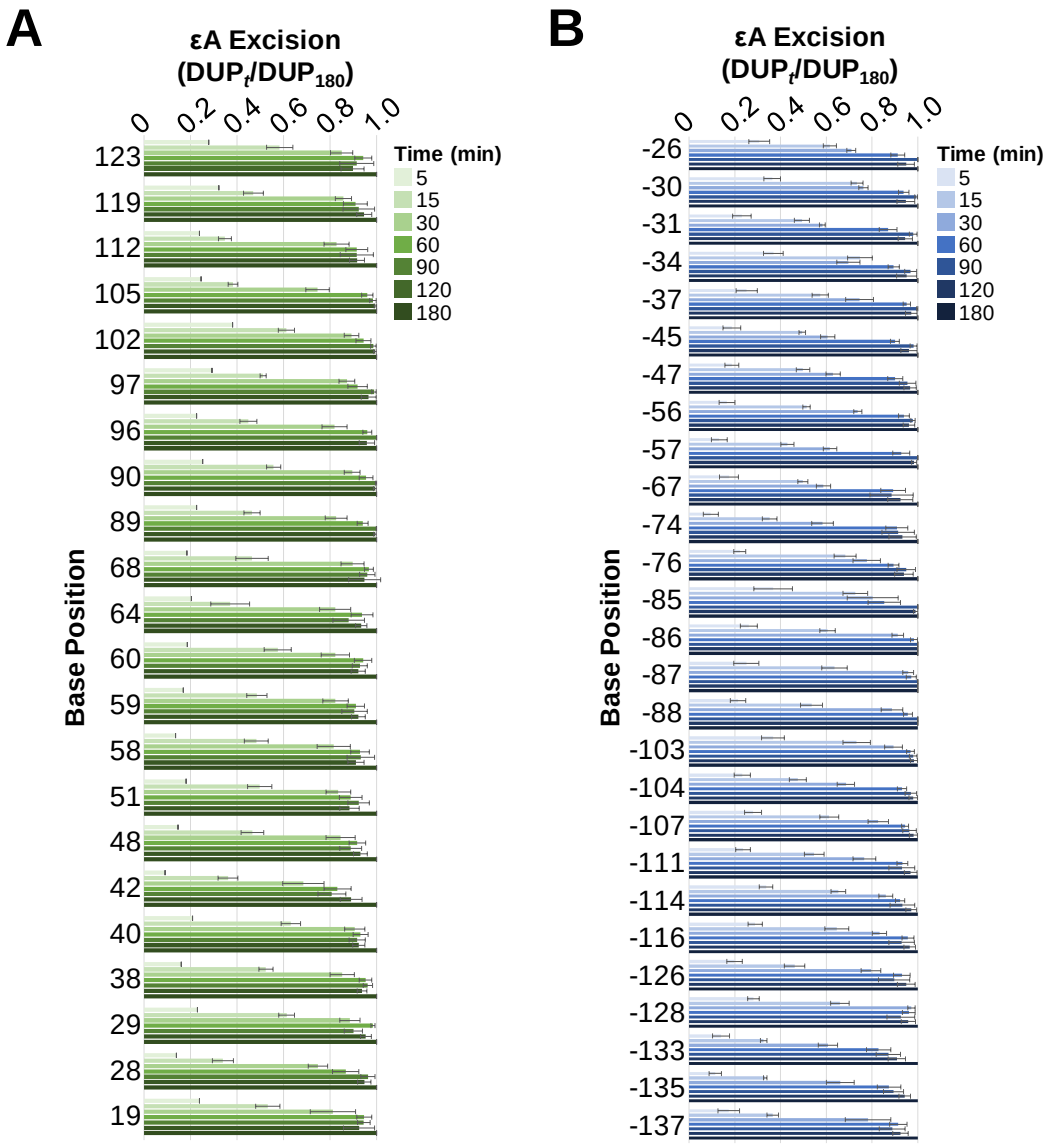

Figure S4. Quantitation of εA excision over time in global DUP. Lesions removed from the (**A**) I strand and (**B**) J strand at the position locations indicated. Product accumulation at time *t* is represented as a ratio relative to product accumulation at 180 min (DUP_t/DUP_{180}), the defined maximal product. Error bars are calculated standard errors (n= 3-10).

Figure S5. Formation of global εA-containing DUP and NCPs.

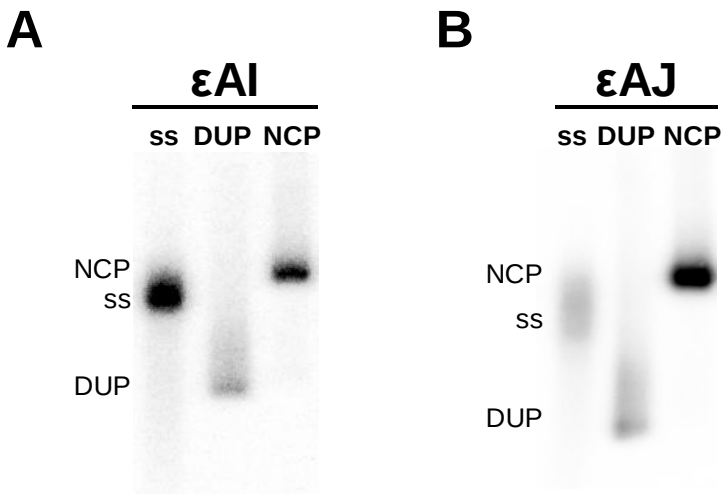

Figure S5. Formation of global εA-containing DUP and NCPs. Representative native PAGE gels showing differential migrations of global εA-containing single-strand (ss), DUP, and NCPs on the (**A**) I strand and (**B**) J strand. When εA was in the I strand it was paired with the J strand lacking damage. When εA was in the J strand, it was paired with I strand lacking damage. Only DUP preparations having ≤ 5% single-strand DNA were used in further studies. Similarly, only NCP preparations having ≤ 5% DUP were used in further studies.

Figure S6. Quantitative assessment of relative AAG activity in NCPs.

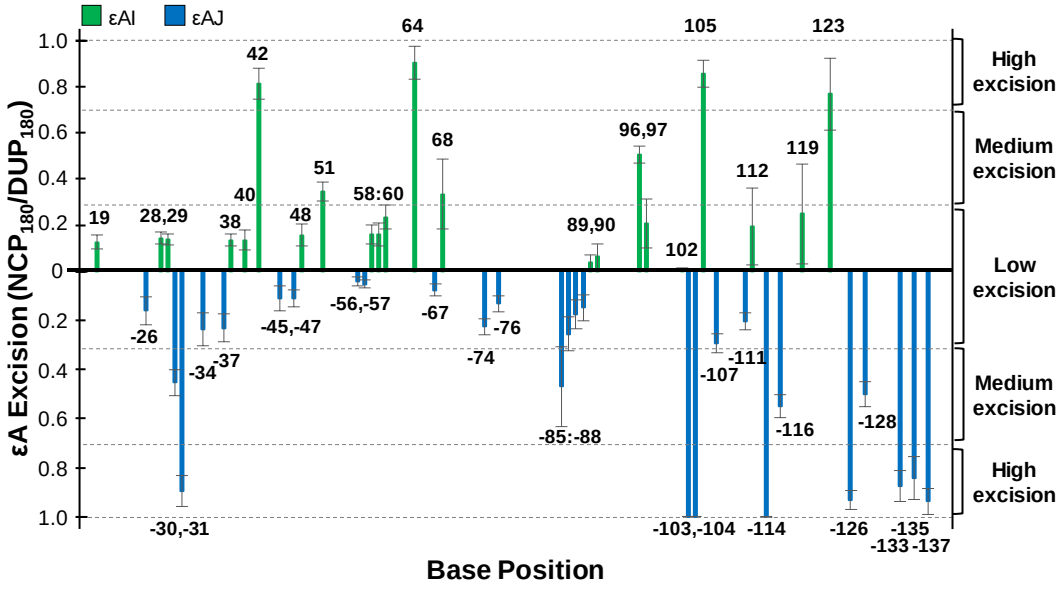

Figure S6. Quantitative assessment of relative AAG activity in NCPs. Relative AAG activity at each NCP position was categorized based on the average product accumulation after 180 min. Low εA excision is defined as product accumulation < 0.3, medium εA excision ranges between 0.3-0.7, and high εA excision is defined as > 0.7. A ratio of 1 represents full repair in NCPs as seen in DUP. Error bars are calculated standard errors (n= 3-10).

Figure S7. Non-biased incorporation of εA-containing DNA into NCPs.

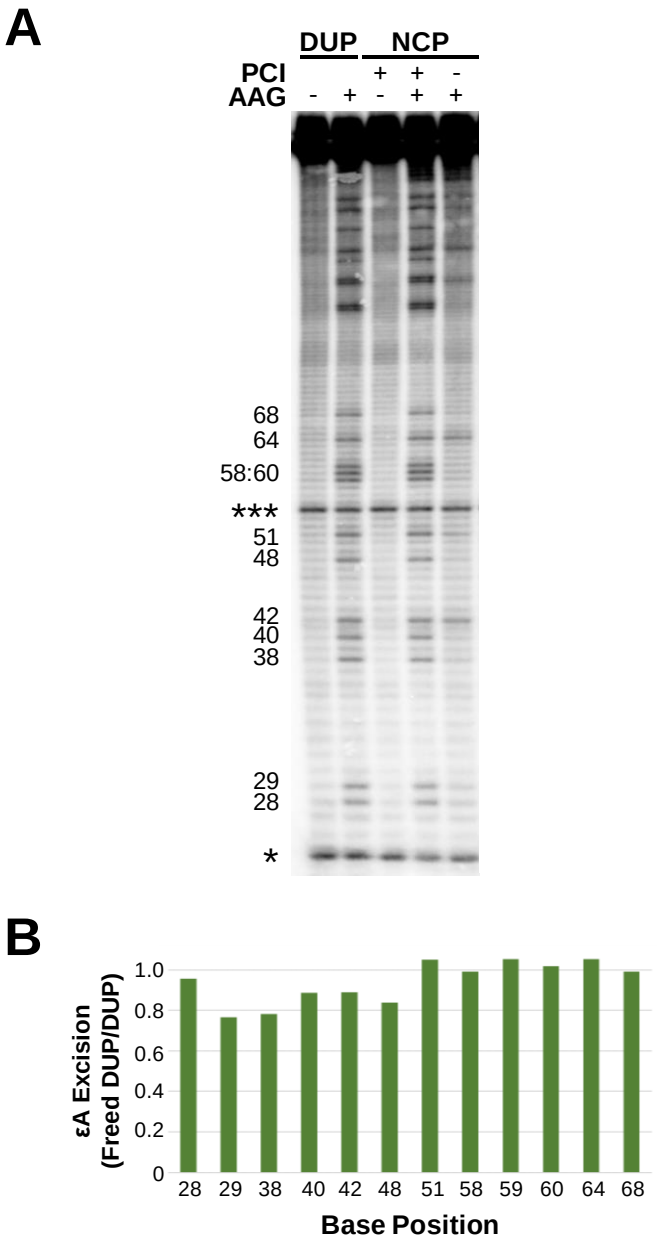

Figure S7. Non-biased incorporation of εA-containing DNA into NCPs. NCPs were assembled with global εA-containing I strand DUP, and then separated from histone octamers using a PCI extraction to create "freed DUP." AAG was incubated with freed DUP for 2 h at 37 °C and with DUP never incorporated into an NCP to compare differences in AAG activity. Different amounts of εA excision between the two samples would suggest biased incorporation of εA lesions during NCP reconstitution. (**A**) Denaturing PAGE gel of reactions for quantitative comparison. Two internal references, a 23 mer (*) and 53 mer (***) used for quantitation are indicated. – AAG lanes were only treated with NaOH to show any damage due to experimental conditions and workup. The freed DUP samples are indicated with + PCI designations. (**B**) Quantification of εA excision in each DUP substrate. A ratio of 1 indicates that the amount of cleavage in the freed DUP is equal to that in the unincorporated DUP.

Figure S8. HRF denaturing PAGE gels to characterize nucleobase solution accessibilities in global εA-containing NCPs shown in **Figure 3** of the main text.

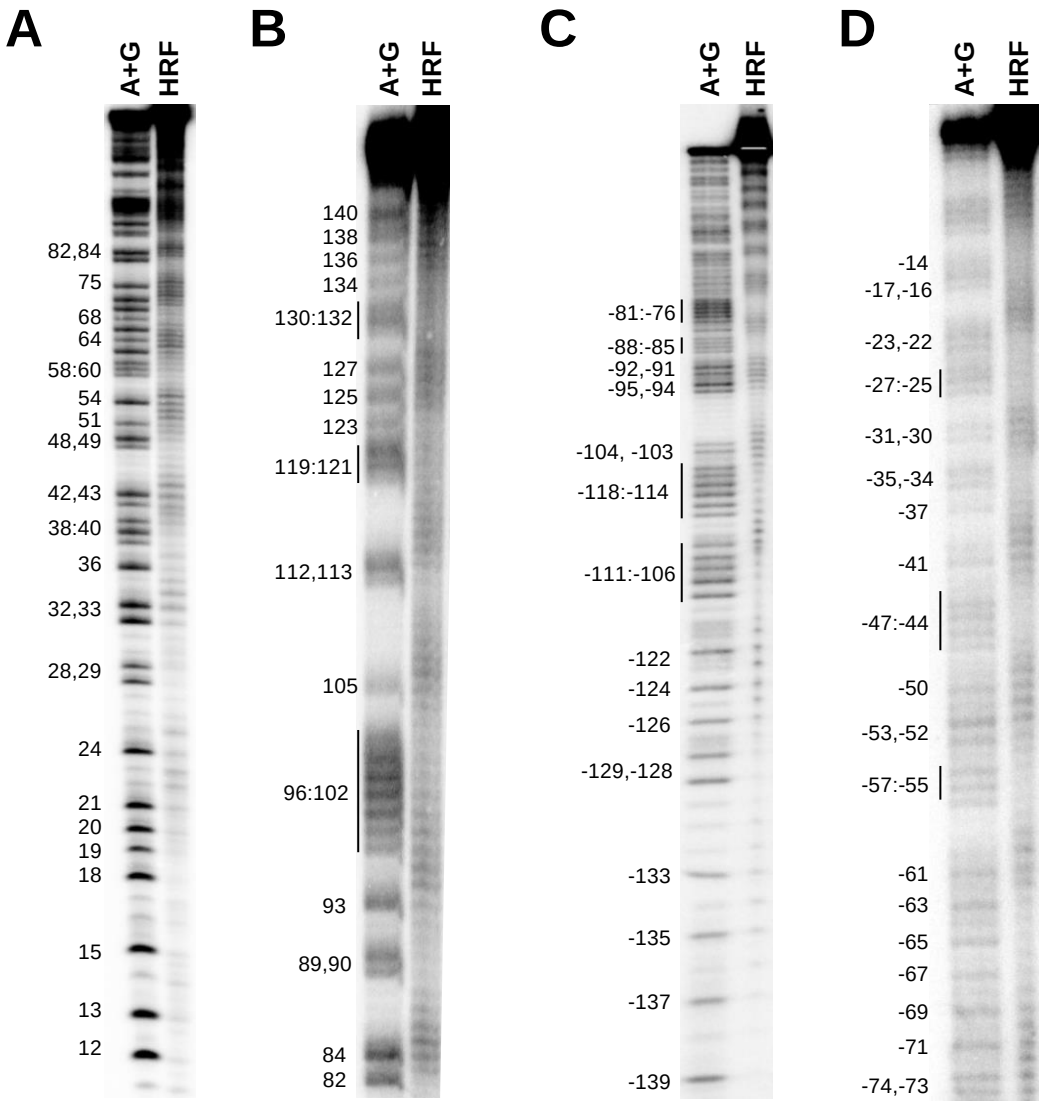

Figure S8. HRF denaturing PAGE gels to characterize nucleobase solution accessibilities in global εA-containing NCPs shown in **Figure 3** of the main text. The HRF reaction on the global εA-containing I strand NCPs of the (**A**) 5′-end and (**B**) 3′-end are shown in the respective HRF lanes. The HRF reaction on the global εA-containing J strand NCPs of the (**C**) 5′-end and (**D**) 3′-end are shown in the respective HRF lanes. The A+G lanes display a sequence ladder created using Maxam-Gilbert reactions using undamaged Widom 601 sequences.

Figure S9. DNase I footprinting on 601I DUP and NCPs.

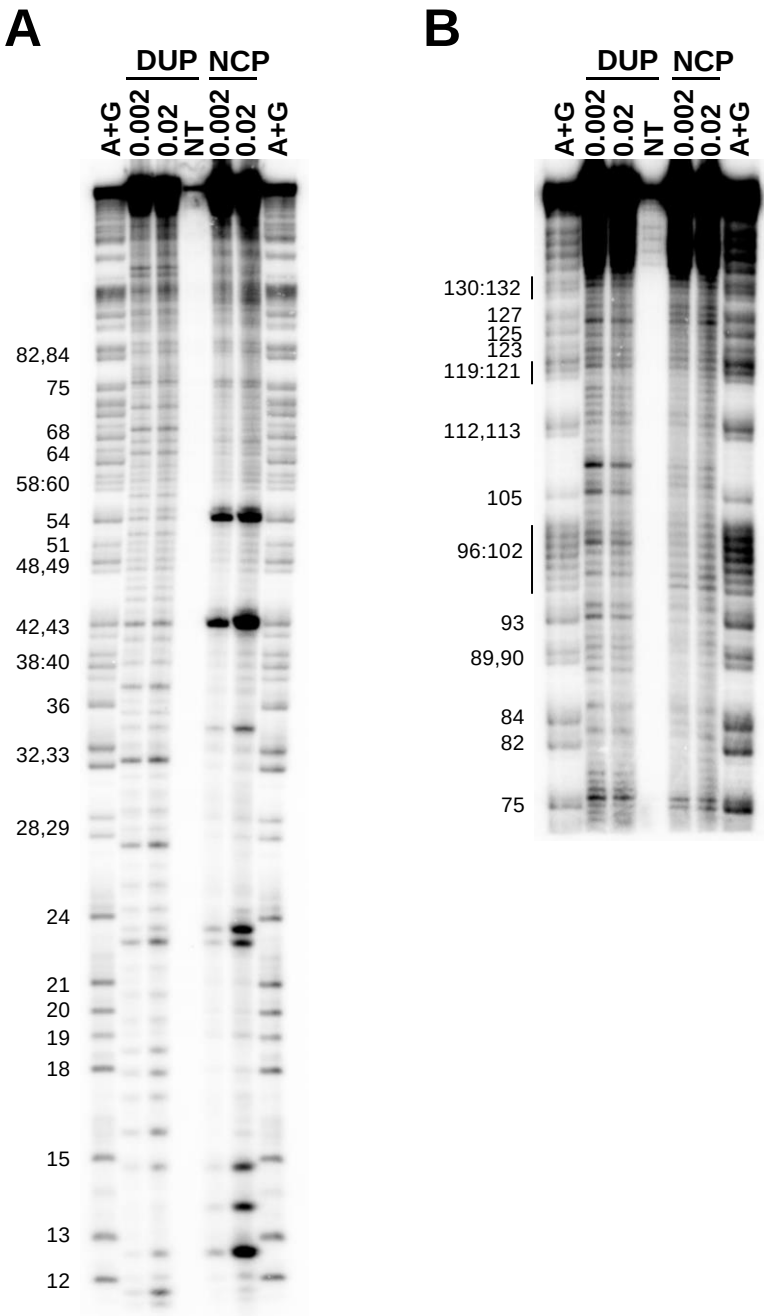

Figure S9. DNase I footprinting on 601I DUP and NCPs. The DNase I footprinting reaction on the (**A**) 5′-end and (**B**) 3′-ends. DNA substrates (2.5 pmol) were reacted with 0.002 U or 0.02 U of DNase I, as indicated. The NT lane is an untreated DUP loaded for reference. A+G lanes are Maxam-Gilbert sequencing reactions, whose products (labeled on the left side of each gel) migrate about 1 nt faster than their analogous DNase I cleavage products.

Figure S10. DNase I footprinting on 601J DUP and NCPs.

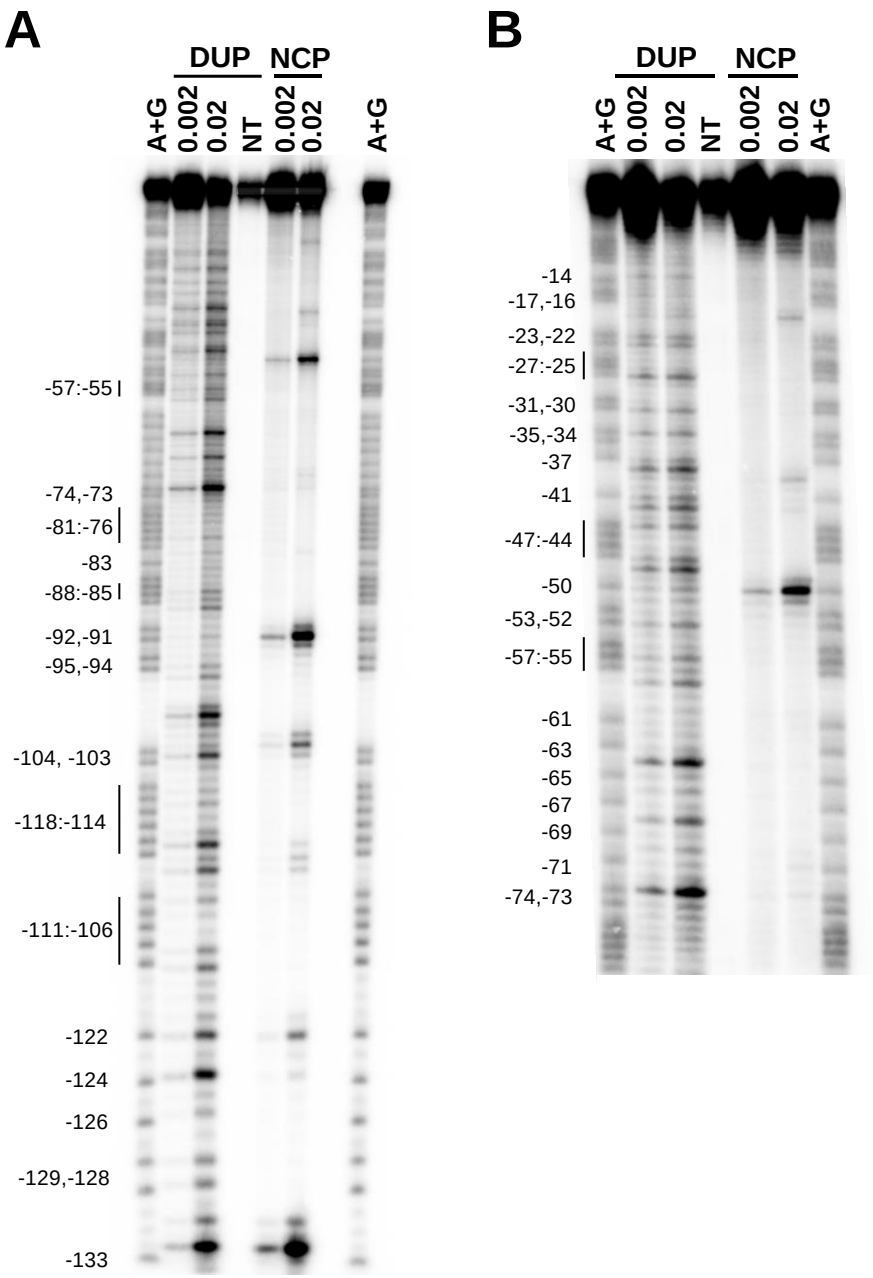

Figure S10. DNase I footprinting on 601J DUP and NCPs. The DNase I footprinting reaction on the (**A**) 5′-end and (**B**) 3′-ends. DNA substrates (2.5 pmol) were reacted with 0.002 U or 0.02 U of DNase I, as indicated. A+G lanes are Maxam-Gilbert sequencing reactions, whose products (labeled on the left side of each gel) migrate about 1 nt faster than their analogous DNase I cleavage products.

Figure S11. DNase I activity in NCPs.

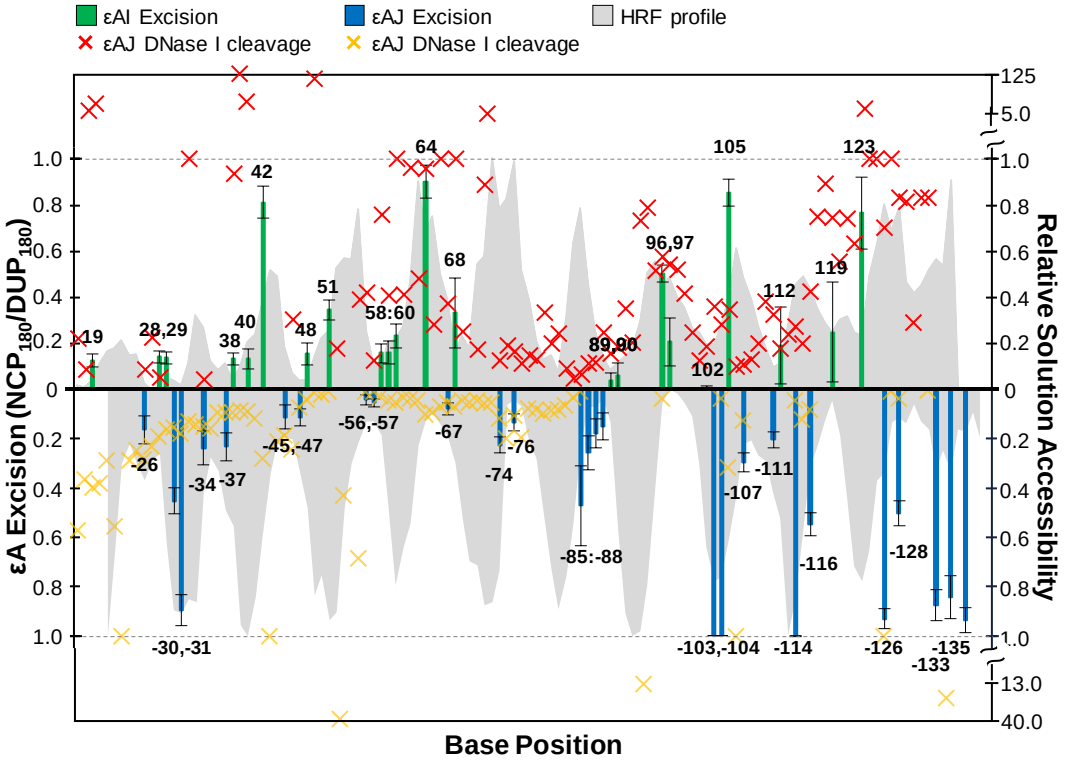

Figure S11. DNase I activity in NCPs. Quantification of DNase I footprinting of the 601I strand (red crosses; **Figure S9**) and the 601J strand (yellow crosses; **Figure S10**) in NCPs is compared with AAG excision (green and blue bars) and HRF profile (gray area). DNase I activity and the HRF profile share the y-axis on the right. Sites where DNase I cleavage was relatively high are indicated with a break in the y-axis on the right.

Figure S12. Proximity of histone tails to HIGH positions with low AAG activity.

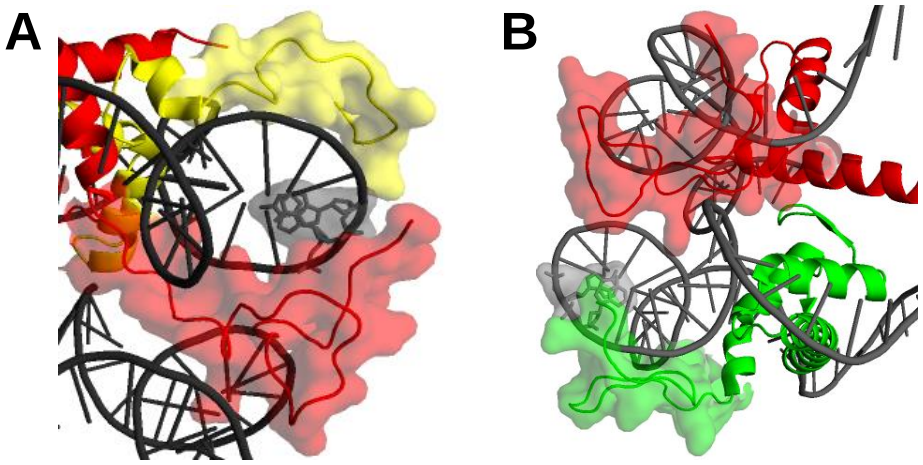

Figure S12. Proximity of histone tails to HIGH positions with low AAG activity. Zoom-in views of NCP crystal structure showing proximity of histone tails that may be within the potential area of effect on HIGH positions with decreased AAG activity. (**A**) Positions -30 and -31 (shown as gray sticks with a surface overlay) are in proximity to the nearby tails of H2A (yellow) and/or H2B (red). (**B**) Positions 96 and 97 (shown as gray sticks with a surface overlay) are similarly near the tails of H4 (green) and H2B (red). Only the histones and lesion-containing strand are shown for simplicity. The histone tails are shown with a surface overlay for emphasis. A merged NCP crystal structure of the Widom 601 duplex (PDB code 3lz0) and histone octamer with tails (PDB 1kx5) was created for these images using PyMOL.

Table S1. k_{obs} values for εA excision by AAG.

Base Position	DUP k_{obs} (min^{-1})	DUP Frac. pdt.	DUP R^2 fit	NCP k_{obs} (min^{-1})	NCP Frac. pdt.	NCP R^2 fit
19	0.057	0.965	0.991	0.044	0.133	0.817
-26	0.060	0.965	0.955	n. d.	< 0.18	n. d.
28	0.037	0.990	0.977	0.019	0.157	0.950
29	0.067	0.970	0.977	0.054	0.139	0.932
-30	0.086	0.954	0.933	0.017	0.435	0.705
-31	0.038	0.979	0.967	0.009	1.092	0.949
-34	0.089	0.930	0.861	n. d.	< 0.240	n. d.
-37	0.054	0.988	0.992	n. d.	< 0.240	n. d.
38	0.054	0.982	0.979	0.073	0.146	0.884
40	0.070	0.957	0.970	0.087	0.167	0.727
42	0.036	0.930	0.964	0.027	0.880	0.966
-45	0.038	0.991	0.983	n. d.	< 0.120	n. d.
-47	0.040	0.984	0.988	n. d.	< 0.120	n. d.
48	0.051	0.958	0.963	0.070	0.171	0.842
51	0.055	0.943	0.970	0.052	0.443	0.785
-56	0.046	0.990	0.995	n. d.	< 0.055	n. d.
-57	0.034	1.020	0.992	n. d.	< 0.065	n. d.
58	0.050	0.965	0.974	n.d.	< 0.220	n. d.
59	0.052	0.955	0.977	0.073	0.156	0.907
60	0.059	0.960	0.984	0.068	0.201	0.785
64	0.046	0.964	0.949	0.038	0.953	0.962
-67	0.039	0.952	0.971	n. d.	< 0.085	n. d.
68	0.053	0.990	0.963	n. d.	< 0.335	n. d.
-74	0.031	0.994	0.987	0.015	0.232	0.866
-76	0.068	0.948	0.965	n. d.	< 0.230	n. d.
-85	0.088	0.951	0.925	0.008	0.660	0.786
-86	0.065	1.007	0.993	0.009	0.322	0.728
-87	0.070	1.007	0.983	n. d.	< 0.190	n. d.
-88	0.056	1.007	0.987	n. d.	< 0.150	n. d.
89	0.048	1.005	0.989	n. d.	< 0.130	n. d.
90	0.060	1.001	0.989	0.045	0.066	0.911
96	0.048	1.000	0.984	0.023	0.621	0.867
97	0.059	0.983	0.976	0.036	0.187	0.852
102	0.076	0.983	0.973	n. d.	< 0.070	n. d.
-103	0.091	0.980	0.997	0.032	0.998	0.928
-104	0.043	0.993	0.994	0.021	1.068	0.974
105	0.041	1.013	0.980	0.021	0.899	0.942
-107	0.065	0.977	0.998	0.009	0.370	0.749
-111	0.054	0.969	0.995	0.007	0.292	0.718
112	0.046	0.963	0.938	n. d.	< 0.193	n. d.
-114	0.079	0.957	0.988	0.023	1.015	0.957
-116	0.071	0.964	0.993	0.010	0.677	0.808
119	0.059	0.958	0.950	n. d.	< 0.260	n. d.
123	0.068	0.945	0.981	0.012	0.854	0.975
-126	0.049	0.964	0.983	0.019	1.025	0.976
-128	0.080	0.976	0.970	0.017	0.537	0.887
-133	0.031	0.965	0.991	0.021	0.939	0.963
-135	0.033	0.982	0.988	0.031	0.944	0.945
-137	0.043	0.962	0.965	0.053	0.971	0.969

Table S1. k_{obs} values for εA excision by AAG. Product accumulation over time was characterized by monophasic kinetic fits by Kaleidagraph to yield k_{obs} and fraction product values for εA positions on the I strand (green rows) and J strand (blue rows) of the global εA-containing DNA substrates. Fields displaying "n.d." were unable to be determined based on the small amounts of product accumulation observed.

Table S2. Solution accessibilities of A positions in NCPs.

Solution Accessibility	HRF Ratio[a]	Positions
LOW	< 0.3	19, -26, 28, 29, 38, -45, 48, -56, -57, 58, 59, 60, -67, 68, -76, -86, -87, 88, 89, 90, -107, 112, 123, -128
MID	0.3-0.7	-34, -37, 40, -47, 51, -85, 102, -111, -116, 119, -126, -137
HIGH	> 0.7	-30, -31, 42, 64, -74, 96, 97, -103, -104, 105, -114, -133, -135

[a] The HRF ratio is the ratio of band intensity at a given cleavage fragment in the HRF profile relative to the highest band intensity within the associated helical turn. This ratio represents the amount of solution accessibility of the nucleobase position relative to the most solution-accessible nucleobase position within the helical turn. LOW was defined as having a ratio of less than 0.3, MID as 0.3-0.7, and HIGH as more than 0.7.

MATERIALS AND METHODS

Global εA-containing 145 mer oligonucleotide synthesis and purification. All oligonucleotides used in this study were synthesized on a MerMade 4 DNA synthesizer (BioAutomation). All phosphoramidites and reagents were purchased from Glen Research. We utilized the 145 bp Widom 601 nucleosome positioning sequence for duplex and NCP assembly (**Scheme S1**).[2] Base pairs are numbered starting from the 5′-end of the I strand, with the J strand designated with a negative (-) (**Figure 1C**). The 145 mer oligonucleotides containing global εA were synthesized on 1,400 Å controlled pore glass beads using phosphoramidites with ultramild protecting groups and deprotected according to the manufacturer's specifications. εA was substituted for A throughout the DNA on either the I strand or J strand of the Widom 601 sequence to ultimately have at most one εA:T bp per DUP. To accomplish this, we used methods similar to our recent report.[3] Briefly, a mixture of εA and A phosphoramidites was used during the synthesis with the molar ratio determined by the Poisson distribution ($\lambda = 0.355$), such that 95% of the DNA population contains either 0 or 1 εA lesion per 145 mer oligonucleotide. The final trityl group was removed on the synthesizer. The DNA was cleaved from the beads by incubation in NH_4OH at room temperature for 2 h and purified by 8% denaturing PAGE run for 5 h at 80 W. A small portion of the synthesized DNA was radiolabeled and was loaded in lanes adjacent to where the unlabeled DNA was loaded. The region of the gel that co-migrated with a 145 mer standard was excised and "crushed and soaked"[4] overnight in 15 mL elution buffer (300 mM sodium acetate [pH 8.0], 1 mM EDTA) with gentle shaking (80 rpm) at 37 °C. The buffer containing the eluted DNA was passed through a 0.22 μm cellulose acetate syringe filter and was concentrated and desalted with many ethanol precipitations. The concentrations of the PAGE-purified oligonucleotides were determined by their absorbance at 260 nm using molar extinction coefficients for the undamaged Widom 601 sequences obtained using the OligoAnalyzer tool on www.idtdna.com.

The incorporation of εA at A sites was confirmed by cleavage by AAG. Specifically, the εA-containing 145 mer strand was 5′-radiolabeled using T4 kinase (New England Biolabs) and γ-^{32}P-ATP (Perkin Elmer) and annealed to its respective undamaged complement to form duplex (see below). The εA-containing duplex (DUP) was then incubated with AAG for 1 h at 37 °C, followed by the addition of equal volume of 1 M NaOH and incubation at 90 °C for 3 min. Samples were supplemented with 40 μL co-precipitation agent (0.5 mg/mL tRNA in 300 mM NaOAc [pH 8.0], 1 mM EDTA) and subsequently desalted with two ethanol precipitations. Samples were prepared for

separation on 12% denaturing PAGE in a 1:1 mixture of formamide and water. Cleavage at each A position confirms that the εA lesions are present as expected (**Figure S1**).

Ligation strategy to synthesize undamaged 145 mer oligonucleotides complementary to εA-containing strands.

The 145 mer oligonucleotides complementary to the εA-containing oligonucleotides were prepared by ligating short component oligonucleotides. The component oligonucleotides for ligation were synthesized using standard phosphoramidite protecting groups with the final trityl group retained for reverse-phase HPLC purification at 90 °C (Agilent PLRP-S column, 250 mm × 4.6 mm; A = 100 mM triethylammonium acetate [TEAA] in 5% aqueous MeCN, B = 100 mM TEAA in MeCN; 5:95 to 35:65 A:B over 30 min, 35:65 to 5:95 A:B over 5 min at 1 mL/min). The trityl group was then removed with incubation in 20% v/v aqueous glacial acetic acid for 1 h at room temperature, followed by a second HPLC purification at 90 °C (Agilent PLRP-S column, 250 mm × 4.6 mm; A = 100 mM triethylammonium acetate [TEAA] in 5% aqueous MeCN, B = 100 mM TEAA in MeCN; 0:100 to 15:85 A:B over 35 min, 15:85 to 35:65 A:B over 5 min at 1 mL/min). Electrospray ionization mass spectrometry was used to verify the identity of the component oligonucleotides.

Component oligonucleotides were used in ligation (**Scheme S2**). Five nmol of each component oligonucleotide 2 and 3 were 5′-phosphorylated in the presence of 2 mM ATP using T4 kinase (New England Biolabs). Phosphorylated component oligonucleotides were combined in equal amounts with component 1 and a 5% excess of two scaffolding oligonucleotides, s12 and s23, in annealing buffer (10 mM Tris-HCl pH 8.0, 50 mM NaCl, 1 mM EDTA). The strands were annealed by heating to 90 °C for 5 min followed by cooling to room temperature at a rate of 1 °C/min. The annealed component oligonucleotides were ligated together overnight at room temperature using T4 ligase (New England Biolabs). The ligated 145 mer oligonucleotides were purified by denaturing PAGE as described above for the εA-containing 145 mer.

Formation of global εA-containing duplex (DUP). The 145 mer oligonucleotides containing εA lesions were 5′-radiolabeled for visualization. The global εA-containing I strand was annealed with the J strand 145 mer that lacked εA lesions. Similarly, the J strand oligonucleotide containing εA lesions was annealed with the undamaged I strand. DUP was formed by mixing the radiolabeled εA-containing strand with the complementary strand in a 1:1.07 ratio

in annealing buffer and heating to 90 °C for 5 min followed by cooling to room temperature at a rate of 1 °C/min. DUP formation was confirmed on a 7% native PAGE (60:1 acrylamide : bisacrylamide; 0.25x TBE). The samples were loaded using 5% (v/v) glycerol in 10 mM Tris-HCl (pH 7.5), 1mM EDTA and run for 3 h at 160 V at 4 °C (**Figure S5 A,B**). Only DUP containing ≤ 5% single-strand DNA were used in further studies.

Reconstitution of global εA nucleosome core particles (NCPs). Recombinant *Xenopus laevis* histones were individually expressed and purified, and subsequently assembled into octamers.[5,6] NCPs were reconstituted by dialyzing the radiolabeled εA-containing DUP population and histone octamer together via salt gradient, as described previously.[3] Briefly, a 10% molar excess of histone octamer was gently added to 25 μL of 1 μM radiolabeled εA-containing 145 bp DUP in buffer (10 mM Tris-HCl [pH 7.5], 1 mM EDTA, 1 mM dithiothreitol [DTT], 2 M NaCl, 500 μg/mL BSA) in a Slide-a-Lyzer dialysis device (0.1 mL capacity, 3.5 kDa MWCO; Thermo Fisher Scientific). The dialysis device started in a buffer of 10 mM Tris-HCl (pH 7.5), 1 mM EDTA, 1mM dithiothreitol (DTT), 2 M NaCl at 4 °C. At 1 h intervals, the device was placed in analogous buffers containing decreasing concentrations of NaCl (1.2 M, 1.0 M, 0.6 M, 0 M). The final dialysis in 0 M NaCl proceeded for 3 h before the reconstitution was filtered with a 0.22 μm cellulose acetate centrifuge tube filter (Corning Costar) to remove precipitates. NCP formation and relative purity were analyzed using a 7% native PAGE (60:1 acrylamide: bisacrylamide; 0.25x TBE) run for 3 h at 160 V in 4 °C (**Figure S5 A,B**). Only NCPs containing ≤ 5% DUP were used in further studies. In this work, the upper limit of contaminating DUP used in NCP experiments is the lowest amount of εA excision observed at a single site. Site -56 has an average product accumulation of 4% (**Figure S6**). Therefore, DUP cannot account for more than 4% of the reported NCP product.

We tested for bias of εA incorporation into NCPs to address the concern of εA enrichment or depletion as a function of εA location. We reconstituted global εA-containing DUP into NCPs and then subsequently removed the histone proteins by extraction with an equal volume of 25:24:1 phenol:chloroform:isoamyl alcohol (PCI) and subsequent ethanol precipitation to create "freed DUP". The freed DUP was incubated with a 30-fold excess of AAG for 2 h at 37 °C in 20 mM Tris-HCl (pH 7.6), 50 mM NaCl, 150 mM KCl, 1 mM EDTA, 1 mM DTT, 200 μg/mL BSA. Samples were quenched with the addition of an equal volume of 1 M NaOH supplemented with internal references (**Scheme S3**). An equal volume of PCI was added and the aqueous layer was subjected to two ethanol

precipitations. The samples were prepared in a 1:1 mixture of formamide and water for separation on a 12% denaturing PAGE to resolve the 5′ end of εA positions (ranging from 28-68) (**Figure S7A**). Quantitation of band intensity was determined by SAFA.[7] The density measurements for all lanes was normalized to the internal references; the 23 mer internal reference was used for the 5′-ends of the sequences (ranging from fragment lengths 9-68) and the 92 mer internal reference was used for the 3′-ends of the sequences (ranging from fragment lengths 70-132). The amount of background damage from the -E sample was subtracted from AAG-treated samples. The resulting amount of cleavage due to AAG activity observed in the freed DUP substrate was compared with analogous conditions of the same DUP population that had never been incorporated into NCPs. The ratio of εA excision in the freed DUP substrate was compared with εA excision in the unincorporated DUP to quantify equal distribution of εA lesions across the NCP populations (**Figure S7B**). A ratio of 1 indicates that the amount of cleavage in the freed DUP is equal to that in the unincorporated DUP, and therefore present in equal amounts in both DUP substrates.

Hydroxyl radical footprinting (HRF). HRF was carried out using previously-published conditions to establish relative solution accessibility of nucleobase positions in NCPs under single-hit conditions.[8,9] Briefly, 7.5 μL of each 1 mM Fe(II)-EDTA, 10 mM sodium ascorbate, and 0.12% w/v aqueous hydrogen peroxide were gently combined with 5 pmol NCPs in a total of 52.5 μL buffer (10 mM Tris-HCl [pH 7.5], 1 mM EDTA). The reaction proceeded at room temperature for 10 min in the dark and was quenched with the addition of 16 μL 50 mM EDTA in 25% v/v glycerol. The quenched sample was immediately loaded onto a 7% native PAGE (60:1 acrylamide: bisacrylamide; 0.25x TBE) and run for 3 h at 160 V at 4 °C. Gel bands containing the NCP species were excised and NCPs were eluted into buffer (0.3 M NaOAc, 1 mM Tris-HCl [pH 8.0], 1 mM EDTA) for 16-20 h at 37 °C with gentle shaking (80 rpm). The NCP eluent was concentrated using a centrifugal concentrator (Sartorius Vivaspin Turbo 15, 5 kDa MWCO) and filtered using a 0.22 μm cellulose acetate centrifuge tube filter (Corning Costar). The sample was extracted twice with equal volume additions of PCI to remove histone proteins, and the resulting aqueous phase was concentrated by SpeedVac evaporation. Following the addition of 40 μL co-precipitation agent (0.5 mg/mL tRNA in 300 mM NaOAc [pH 8.0], 1 mM EDTA), samples were desalted with two ethanol precipitations. Samples were prepared in a 1:1 mixture of formamide and water for denaturing PAGE. Cleavage fragments were resolved after splitting the sample into two halves. Each half was loaded onto separate denaturing PAGE (12% gel for 5′-end

fragments, 8% for 3′-end fragments). Denaturing PAGE were visualized by phosphorimagery (Bio-Rad PharosFX) (**Figure S8**).

Bands resulting from HRF cleavage were quantitated using SAFA gel analysis software.[7] The more solution-accessible a nucleobase position is to hydrogen abstraction, the stronger the intensity of the corresponding cleavage fragment. Categorization of solution accessibilities of nucleobases were determined as a ratio of band intensity at a given position relative to the highest band intensity within the helical turn. Highly solution-accessible (HIGH) positions were defined as those with a ratio greater than 0.7; medium solution-accessible (MID) positions with a ratio range from 0.3-0.7; solution-inaccessible (LOW) positions were defined as those with a ratio less than 0.3 (**Table S2**).

DNase I footprinting of NCPs. NCPs were reconstituted using DUP containing no εA lesions (in 10 mM Tris-HCl [pH 7.5], 1 mM EDTA, 1 mM dithiothreitol [DTT], 2 M NaCl, 500 μg/mL BSA) and were treated with varying amounts of DNase I (New England Biolabs). 2.5 pmol NCP (containing <2% DUP determined by native PAGE) were incubated with 0.02 and 0.002 U DNase I at 37 °C for 5 min in 1x DNase I buffer (10 mM Tris·HCl, 7.5 mM $MgCl_2$, 0.5 mM $CaCl_2$, pH 7.6) supplemented with an additional 10 mM $MgCl_2$ for a final concentration of 17.5 mM $MgCl_2$. The reaction was quenched with the addition of one-third the reaction volume of 50 mM EDTA–0.5% sodium dodecyl sulfate (SDS)–0.2 mg/ml proteinase K, followed by incubation at 50°C for 2 h. Protein extraction was performed with equal volume additions of PCI, followed by two ethanol precipitations.

As a control, DNase I footprinting was performed on DUP in analogous buffer conditions, but incubated at 37 °C for 2 min. The reaction was quenched with the addition of half the reaction volume of 100 mM EDTA-1 mg/mL calf-thymus DNA. Samples were ethanol precipitated twice.

All samples were prepared in a 1:1 mixture of formamide and water for denaturing PAGE similar to those described for HRF above. Denaturing PAGE were visualized by phosphorimagery (Bio-Rad PharosFX) (**Figure S9, S10**). Bands resulting from DNase I cleavage were quantitated using SAFA gel analysis software.[7] Similar to HRF, the more solution accessible a nucleobase position is for cleavage, the stronger the intensity of the corresponding cleavage fragment. Relative DNase I activity was determined as a ratio of band intensity at a given position relative to the

median band intensity of the local helical turn maxima. Highly cleaved positions are graphed with a break in the y-axis of **Figure S11**.

AAG kinetics on global εA-containing DNA. AAG was purchased from New England Biolabs. The total concentration of AAG was determined by the Bradford method using bovine γ-globulin standards (Bio-Rad Laboratories). All AAG concentrations given below or in figure captions are total enzyme concentrations.

Reactions were initiated after the DNA substrate and AAG were pre-equilibrated at 37 °C for 2 min by combining an equal volume of 26.6 nM DNA substrate (DUP or NCP) and 0.8 μM AAG for a final experimental sample of 13.3 nM DNA and 0.4 μM AAG in 20 mM Tris-HCl (pH 7.6), 50 mM NaCl, 150 mM KCl, 1 mM EDTA, 1 mM DTT, 200 μg/mL BSA. The reactions were incubated at 37 °C for 5, 15, 30, 60, 90, 120, or 180 min before they were quenched with an equal volume of 1 M NaOH supplemented with the radiolabeled internal references and incubated at 90 °C for 3 min. Timepoints were initiated in such a way that all samples were quenched at the same time before immediate sample workup; this process was used to avoid extended incubation of εA lesions in NaOH after quenching which could result in degradation and false-positive results of AAG-catalyzed cleavage.[12,13] After incubation with NaOH, an equal volume of PCI was added followed by 40 μL of co-precipitation agent (0.5 mg/mL tRNA in 300 mM NaOAc [pH 8.0], 1 mM EDTA) and the samples were subsequently desalted with two ethanol precipitations. The (-E) sample was not incubated with AAG but instead an equivalent volume of reaction buffer was added and incubated at 37 °C for 180 min, quenched, and subsequently worked up like the rest of the samples. Any preexisting damage, such as depurination, or incidental damage due to experimental conditions or workup was revealed by this NaOH treated sample, which was used for a background subtraction for AAG-treated samples. Therefore, the amount of εA excision reported is strictly due to AAG's enzymatic activity.

After the final ethanol precipitation all samples were resuspended in a 1:1 mixture of formamide and water and split in half. Each half was loaded onto separate denaturing PAGE (12% gel for 5′-end fragments; 8% for 3′-end fragments). The PAGE gels were visualized by phosphorimagery on a Bio-Rad PharosFX and quantified by SAFA.[7] The internal references served as a loading control and also allowed us to account for loss of εA cleavage products due to sample workup, especially smaller fragments that have a decreased ability to precipitate.[14] Accordingly, the band intensities in each lane were normalized to an internal reference. The 23 mer internal reference was used for the

5′-end fragments (ranging from 9-68) and the 92 mer internal reference was used for the 3′-ends fragments (ranging from 70-132). After this normalization the band intensity in the -E lane was subtracted from the AAG-treated samples.

As a result of the global lesion substitution, <1% of the DNA population is available as a substrate at each εA position. Therefore, the exposure time needed for phosphorimagery leads to overexposure of the parent band which then cannot be accurately quantified and used as a reference point to determine the amount of cleavage product at each εA. To address this technical challenge, we defined the amount of product observed with the DUP control after 180 min as the theoretical maximum amount of product at a given lesion position (DUP_{180}). Therefore, product accumulation at time *t* is represented as a ratio relative to DUP_{180}. In DUP, product accumulation at time *t* is represented as DUP_t/DUP_{180}, where DUP fraction product is normalized to 1.0 for the 180 min sample. In NCPs, product accumulation at time *t* is represented as NCP_t/DUP_{180}, where a ratio of 1.0 indicates the εA is removed completely, as in DUP. Replicate data at each observed εA position were averaged for every timepoint, and then fit to a single exponential model $y(t) = y_{\max}(1 - e^{-k_{\text{obs}}t})$, where $y_{\max}$ is the amplitude of the reaction's fit (fraction product in **Table S1**), k_{obs} is the observed rate constant, and *t* is time. Error bars shown are calculated standard errors (SE) from 3-10 replicates for each εA position at each timepoint: $SE = \frac{\sigma}{\sqrt{n}}$, where σ is the standard deviation of the population and *n* is the number of replicates.

We confirmed that AAG retains full activity during the 180 min time course (**Figure S3**). The activity of AAG pre-incubated for 180 min (3 h sample) at 37 °C under experimental conditions was compared to that of AAG directly added (0 h sample) to global εA-containing DUP. After addition, the reactions proceeded for 1 h at 37 °C before quenching with NaOH supplemented with radiolabeled internal references and sample workup as described above. Cleavage products resulting from εA excision were resolved on a 12% denaturing PAGE to resolve the 5′-end fragments and quantified by SAFA.[7] After normalization using the 53 mer internal reference and background subtraction of the -E data the ratio of product formation for the 180 min sample relative to the 0 h sample was determined. A ratio of 1 indicates that after 180 min at 37 °C AAG retains full activity.

Molecular modeling of NCP. A crystal structure modeling the Widom 601 sequence wrapped around a *X. laevis* histone octamer with histone tails was created using the "merge" function in PyMOL (**Figure 1B, Figure S12**). The NCP crystal structure containing the Widom 601 sequence but which lacks histone tails (PDB ID: 3lz0) was merged

with an NCP crystal structure containing the alpha-satellite DNA sequence but containing the histone tails (PDB ID: 1kx5) by aligning the overlapping histone protein amino acid sequences. The Widom 601 duplex and the histone octamer containing the histone tails were combined and merged to create a new, separate PyMOL object.

SUPPLEMENTARY REFERENCES

(1) Vasudevan, D., Chua, E. Y. D., and Davey, C. A. (2010) Crystal Structures of Nucleosome Core Particles Containing the “601” Strong Positioning Sequence. *J. Mol. Biol. 403*, 1–10.

(2) Lowary, P. T., and Widom, J. (1998) New DNA sequence rules for high affinity binding to histone octamer and sequence-directed nucleosome positioning. *J. Mol. Biol. 276*, 19–42.

(3) Bilotti, K., Tarantino, M. E., and Delaney, S. (2018) Human Oxoguanine Glycosylase 1 Removes Solution Accessible 8-Oxo-7,8-dihydroguanine Lesions from Globally Substituted Nucleosomes Except in the Dyad Region. *Biochemistry 57*, 1436–1439.

(4) Sambrook, J., and Russell, D. W. (2006) Isolation of DNA Fragments from Polyacrylamide Gels by the Crush and Soak Method. *Cold Spring Harb. Protoc.* (Sambrook, J., and Russell, D., Eds.) *2006*, pdb.prot2936.

(5) Luger, K., Rechsteiner, T. J., and Richmond, T. J. (1999) Expression and purification of recombinant histones and nucleosome reconstitution. *Methods Mol. Biol. 119*, 1–16.

(6) Olmon, E. D., and Delaney, S. (2017) Differential Ability of Five DNA Glycosylases to Recognize and Repair Damage on Nucleosomal DNA. *ACS Chem. Biol. 12*, 692–701.

(7) Das, R., Laederach, A., Pearlman, S. M., Herschlag, D., and Altman, R. B. (2005) SAFA: semi-automated footprinting analysis software for high-throughput quantification of nucleic acid footprinting experiments. *RNA 11*, 344–354.

(8) Hayes, J. J., Tullius, T. D., and Wolffe, A. P. (1990) The structure of DNA in a nucleosome. *Proc. Natl. Acad. Sci. U. S. A. 87*, 7405–7409.

(9) Jain, S. S., and Tullius, T. D. (2008) Footprinting protein–DNA complexes using the hydroxyl radical. *Nat. Protoc. 3*, 1092–1100.

(10) Maxam, A. M., and Gilbert, W. (1977) A new method for sequencing DNA. *Proc. Natl. Acad. Sci. U. S. A. 74*, 560–564.

(11) Maxam, A. M., and Gilbert, W. (1980) Sequencing end-labeled DNA with base-specific chemical cleavages. *Methods Enzymol. 65*, 499–560.

(12) Speina, E., Cieśla, J. M., Wójcik, J., Bajek, M., Kuśmierek, J. T., and Tudek, B. (2001) The Pyrimidine Ring-opened Derivative of 1,N 6-Ethenoadenine Is Excised from DNA by the Escherichia coli Fpg and Nth Proteins. *J. Biol. Chem. 276*, 21821–21827.

(13) Hedglin, M., and O'Brien, P. J. (2008) Human alkyladenine DNA glycosylase employs a processive search for DNA damage. *Biochemistry 47*, 11434–11445.

(14) Shaytan, A. K., Xiao, H., Armeev, G. A., Wu, C., Landsman, D., and Panchenko, A. R. (2017) Hydroxyl-radical footprinting combined with molecular modeling identifies unique features of DNA conformation and nucleosome positioning. *Nucleic Acids Res. 45*, 9229–9243.